Acta Universitatis Apulensis
ISSN: 1582-5329
http://www.uab.ro/auajournal/

No. 71/2022
pp. 117-125
doi: 10.17114/j.aua.2022.71.08

# FREE CONVECTION IN A SQUARE CAVITY FILLED BY A BIDISPERSE POROUS MEDIUM. EFFECT OF INTERNAL HEAT GENERATION

D. Breaz, T. Groşan, F. Pătrulescu, C. Revnic

Abstract. The natural convection in an enclosure filled by a bidisperse porous medium in the presence of internal heat generation is studied. The two velocities - one temperature (thermal equilibrium between the macro- and micro -phases) mathematical model is solved numerically using the finite difference method. For different values of the governing parameters streamlines and isotherms are depicted and maximum values of the stream functions and temperature are reported.

2010 *Mathematics Subject Classification*: 76S05, 76M20, 80A20

*Keywords:* free convection, bidisperse porous medium, numerical results, Darcy model.

## 1. Introduction

In the last years, there has been much interest in transfer phenomena in bidisperse porous media (BDPM). A bidisperse porous medium is formed by voids filled with fluid and a porous matrix composed by clusters of large particles (the macro-phase) that are agglomerations of small particles (the micro-phase) (see, [6], [8]). In order to model the momentum and the energy transfer in a BDPM, [7] proposed a mathematical model with two momentum equations and two temperature equations. Thus, for the transfer phenomena in the macro-phase we need two equations (momentum and energy) while other two equations (momentum and energy) are used for the micro-phase. The momentum and the energy equations are interconnected each other through inter-phases transfer terms. However, in [3] and [4] is reported that when the porosities of the two phase are low, it is possible to consider a local thermal equilibrium between the macro-phase and micro-phase and to use in the mathematical model only one equation for energy. Several other authors studied the transfer phenomena in BDPM, it is worth to mention: [9], [10], [11], [12].
In this paper we study the effect of internal heat generation in a cavity filled by a BDPM with a local thermal equluibrium between the macro and micro phases.

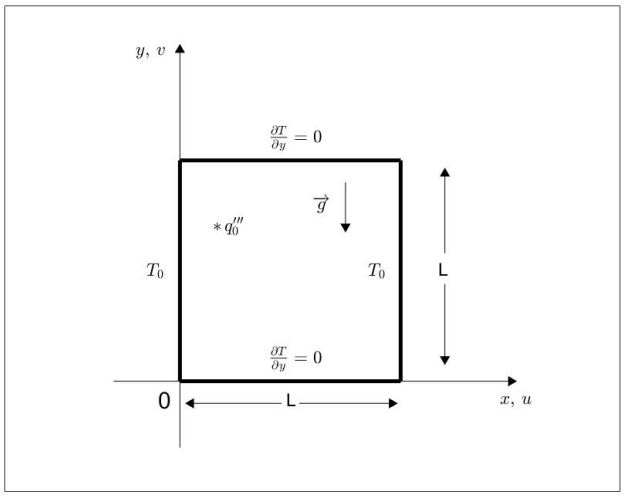


Figure 1: The geometry of the problem

## 2. Basic equations

Consider a square cavity filled by a BDPM in the presence of the internal heat generation. The physical model is depicted in Fig. 1. The mathematical model is given by (see, [4]):
Continuity equations:

$$\frac{\partial u_f}{\partial x} + \frac{\partial v_f}{\partial y} = 0 \tag{1}$$

$$\frac{\partial u_p}{\partial x} + \frac{\partial v_p}{\partial y} = 0 \tag{2}$$

Momentum equations:

$$\frac{\partial p}{\partial x} = -\frac{\mu}{K_f} u_f - \zeta(u_f - u_p) \tag{3}$$

$$\frac{\partial p}{\partial y} = -\frac{\mu}{K_f} v_f - \zeta(v_f - v_p) + \rho g \hat{\beta}(T - T_0) \tag{4}$$

$$\frac{\partial p}{\partial x} = -\frac{\mu}{K_p} u_p - \zeta(u_p - u_f) \tag{5}$$

$$\frac{\partial p}{\partial y} = -\frac{\mu}{K_p} v_p - \zeta(v_p - v_f) + \rho g \hat{\beta}(T - T_0) \tag{6}$$

Energy equation:

$$(\rho c)_f \Big( \big(\phi\, u_f + (1-\phi)\varepsilon\, u_p\big) \frac{\partial T}{\partial x} + \big(\phi\, v_f + (1-\phi)\varepsilon\, v_p\big) \frac{\partial T}{\partial y} \Big) =$$

$$= k_m \Big( \frac{\partial^2 T}{\partial x^2} + \frac{\partial^2 T}{\partial y^2} \Big) + q_0''' \tag{7}$$

where

$$k_m = (1-\varepsilon) k_s + (\phi + (1-\phi)\varepsilon) k_f \tag{8}$$

$$(\rho c)_m = (1-\varepsilon)(1-\phi)(\rho c)_s + (\phi + (1-\varepsilon)\phi)(\rho c)_f. \tag{9}$$

The boundary conditions are given by (see Fig. 1)

$$u_f = 0,\ u_p = 0,\ T = T_0 \text{ at } x = 0 \text{ and } x = L,\ 0 \le y \le L \tag{10}$$

$$v_f = 0,\ v_p = 0,\ \frac{\partial T}{\partial y} = 0 \text{ at } y = 0 \text{ and } y = L,\ 0 \le x \le L \tag{11}$$

Here $\mu$, $K$, $\zeta$, $\hat{\beta}$, $\rho$, $c$, $\phi$, $\epsilon$, $k_m$, $q_0'''$ are the viscosity, permeability, volumetric expansion coefficient, density, heat capacity, porosity for macro-phase, porosity for micro-phase, thermal conductivity and heat generation term, while the subscripts $f$ and $p$ refers to the macro- and micro -phases.
We eliminate the pressure term using standard arguments and introduce the effective

thermal diffusivity. The governing equations (3)–(7) can be written as

$$-\Big(\frac{\mu}{K_f}+\zeta\Big)\Big(\frac{\partial u_f}{\partial y}-\frac{\partial v_f}{\partial x}\Big)+\zeta\Big(\frac{\partial u_p}{\partial y}-\frac{\partial v_p}{\partial x}\Big)=\rho g\hat{\beta}\frac{\partial T}{\partial x} \tag{12}$$

$$\zeta\Big(\frac{\partial u_f}{\partial y}-\frac{\partial v_f}{\partial x}\Big)-\Big(\frac{\mu}{K_p}+\zeta\Big)\Big(\frac{\partial u_p}{\partial y}-\frac{\partial v_p}{\partial x}\Big)=\rho g\hat{\beta}\frac{\partial T}{\partial x} \tag{13}$$

$$\beta\Big(\big(\phi\, u_f+(1-\phi)\varepsilon\, u_p\big)\frac{\partial T}{\partial x}+\big(\phi\, v_f+(1-\phi)\varepsilon\, v_p\big)\frac{\partial T}{\partial y}\Big)=$$

$$=\alpha_m\Big(\frac{\partial^2 T}{\partial x^2}+\frac{\partial^2 T}{\partial y^2}\Big)+\frac{q_0'''}{(\rho c)_m} \tag{14}$$

where

$$\beta=\frac{(\rho c)_f}{(\rho c)_m},\quad \alpha_m=\frac{k_m}{(\rho c)_m}.$$

Next, we consider the dimensionless variables (see, [5])

$$(X,Y)=\frac{1}{L}(x,y),\ (U_f,U_p)=\frac{L}{\alpha_m}(u_f,u_p),$$

$$(V_f,V_p)=\frac{L}{\alpha_m}(v_f,v_p),\ \Theta=\frac{(T-T_0)}{q_0'''L^2/k_m} \tag{15}$$

and equations (1)–(2) and (12)-(14) have the following dimensionless form

$$\frac{\partial U_f}{\partial X}+\frac{\partial V_f}{\partial Y}=0,\quad \frac{\partial U_p}{\partial X}+\frac{\partial V_p}{\partial Y}=0 \tag{16}$$

$$-(1+\sigma_f)\Big(\frac{\partial U_f}{\partial Y}-\frac{\partial V_f}{\partial X}\Big)+\sigma_f\Big(\frac{\partial U_p}{\partial Y}-\frac{\partial V_p}{\partial X}\Big)=Ra\frac{\partial \Theta}{\partial X} \tag{17}$$

$$\sigma_f\Big(\frac{\partial U_f}{\partial Y}-\frac{\partial V_f}{\partial X}\Big)-\Big(\frac{1}{Kr}+\sigma_f\Big)\Big(\frac{\partial U_p}{\partial Y}-\frac{\partial V_p}{\partial X}\Big)=Ra\frac{\partial \Theta}{\partial X} \tag{18}$$

$$\beta\Big(\big(\phi\, U_f+(1-\phi)\varepsilon\, U_p\big)\frac{\partial \Theta}{\partial X}+\big(\phi\, V_f+(1-\phi)\varepsilon\, V_p\big)\frac{\partial \Theta}{\partial Y}\Big)=$$

$$=\frac{\partial^2\Theta}{\partial x^2}+\frac{\partial^2\Theta}{\partial y^2}+1, \tag{19}$$

where

$$\sigma_f=\frac{K_f\zeta}{\mu},\ K_r=\frac{K_p}{K_f},\ Ra=\frac{\rho g\hat{\beta}K_f\big(q_0'''L^2/k_m\big)L}{\mu\alpha_m}$$

Finally, we introduce the stream functions $\psi_f$ and $\psi_p$ given by (see, [10])

$$(U_f, U_p) = \frac{\partial}{\partial Y}(\psi_f, \psi_p), \quad (V_f, V_p) = -\frac{\partial}{\partial X}(\psi_f, \psi_p) \tag{20}$$

and the governing equations (16)-(19) are transformed in the following nonlinear system

$$-(1+\sigma_f)\Big(\frac{\partial^2\psi_f}{\partial X^2}+\frac{\partial^2\psi_f}{\partial Y^2}\Big)+\sigma_f\Big(\frac{\partial^2\psi_p}{\partial X^2}+\frac{\partial^2\psi_p}{\partial Y^2}\Big)=Ra\frac{\partial\Theta}{\partial X} \tag{21}$$

$$\sigma_f\Big(\frac{\partial^2\psi_f}{\partial X^2}+\frac{\partial^2\psi_f}{\partial Y^2}\Big)-\Big(\frac{1}{Kr}+\sigma_f\Big)\Big(\frac{\partial^2\psi_p}{\partial X^2}+\frac{\partial^2\psi_p}{\partial Y^2}\Big)=Ra\frac{\partial\Theta}{\partial X} \tag{22}$$

$$\beta\Big(\big(\phi\,\frac{\partial\psi_f}{\partial Y}+(1-\phi)\varepsilon\,\frac{\partial\psi_p}{\partial Y}\big)\frac{\partial\Theta}{\partial X}-\big(\phi\,\frac{\partial\psi_f}{\partial X}+(1-\phi)\varepsilon\,\frac{\partial\psi_p}{\partial X}\big)\frac{\partial\Theta}{\partial Y}\Big)=$$

$$=\frac{\partial^2\Theta}{\partial X^2}+\frac{\partial^2\Theta}{\partial Y^2}+1 \tag{23}$$

The boundary conditions (10)–(11) are reduced to

$$\psi_f=\psi_p=0,\ \Theta=0 \ \text{ at } X=0 \text{ and } X=1,\ 0\le Y\le 1 \tag{24}$$

$$\psi_f=\psi_p=0,\ \frac{\partial\Theta}{\partial Y}=0 \ \text{ at } Y=0 \text{ and } Y=1,\ 0\le X\le 1 \tag{25}$$

## 3. Numerical results

In this section we provide and analyze the numerical solutions of nonlinear equations (21)–(23) subject to boundary conditions (24)–(25). First of all, we give the following equivalent form of (21) and (22)

$$\frac{\partial^2\psi_f}{\partial X^2}+\frac{\partial^2\psi_f}{\partial Y^2}=-\frac{1+2\sigma_f Kr}{1+\sigma_f+\sigma_f Kr}Ra\frac{\partial\Theta}{\partial X} \tag{26}$$

$$\frac{\partial^2\psi_p}{\partial X^2}+\frac{\partial^2\psi_p}{\partial Y^2}=-\frac{Kr+2\sigma_f Kr}{1+\sigma_f+\sigma_f Kr}Ra\frac{\partial\Theta}{\partial X} \tag{27}$$

The governing equations (26), (27) and (23) are solved numerically using a central finite difference method of second order along with a SOR iterative technique. We used in our numerical calculations the cluster Kotys (see, [1]). A grid dependency test was done and the chosen grid for these simulations was $101 \times 101$. Moreover, the obtained solution was compared in the case of the monodisperse porous medium

Table 1: Comparison on $\max|\psi|$ and $\max|\Theta|$ for a rectangular cavity with the aspect ratio height/length = 2 filled by a monodisperse porous medium

| $Ra$ | [2] | | [5] | | Present | |
|---|---|---|---|---|---|---|
| | $\max\|\psi\|$ | $\max\|\Theta\|$ | $\max\|\psi\|$ | $\max\|\Theta\|$ | $\max\|\psi\|$ | $\max\|\Theta\|$ |
| 10 | 0.078 | 0.130 | 0.079 | 0.127 | 0.079 | 0.127 |
| $10^3$ | 4.880 | 0.118 | 4.832 | 0.116 | 4.835 | 0.116 |

with that reported by [2] and [5] and a good agreement was obtained, see Table 1. The numerical simulations were performed for several values of the involved parameters. The porosities of the macrophases and microphase were fixed to typical values for usual porous media: $\phi = 0.5$ and $\epsilon = 0.3$ and the ratio $\beta$ at 0.7. The other parameters lies in the ranges: $Ra \in \{10^2, 10^3, 10^4, 10^5\}$, $K_r \in \{10^{-3}, 10^{-1}\}$ and $\sigma_f \in \{0.1, 1\}$.
The variation of the maximum values of the stream functions $\psi_f$ and $\psi_p$ and temperature $\Theta$ is given in Table 2. We notice that the lowest temperature is reached for $Ra = 10^3$, $K_r = 10^{-1}$ and $\sigma_f = 0.1$.

Table 2: Maximum absolute value of streamlines and temperature

| $Ra$ | $K_r$ | $\sigma_f$ | $\max\|\psi_f\|$ | $\max\|\psi_p\|$ | $\max\|\Theta\|$ |
|---|---|---|---|---|---|
| $10^2$ | $10^{-3}$ | 0.1 | 0.6631 | 0.0007 | 0.1302 |
| | | 1 | 0.3670 | 0.0010 | 0.1280 |
| | $10^{-1}$ | 0.1 | 0.6698 | 0.0788 | 0.1304 |
| | | 1 | 0.4183 | 0.1045 | 0.1287 |
| $10^3$ | $10^{-3}$ | 0.1 | 4.9939 | 0.0059 | 0.1271 |
| | | 1 | 3.1977 | 0.0095 | 0.1350 |
| | $10^{-1}$ | 0.1 | 4.9773 | 0.5855 | 0.1262 |
| | | 1 | 3.4915 | 0.8728 | 0.1332 |

Streamlines for the macrophase and microphase and isotherms are depicted in Figs. 2 to 5 for different values of the Rayleigh number, $Ra$. It is observed that two cells of convection are formed in both macro-and micro -phases and the temperature is higher in the middle of the cavity. When Ra increases the streamlines maximum values is located closer to the top corners, while the location of the maximum of the temperature goes closer to the middle of the top wall. This happen because the convection streams push the hotter layers of fluids near the top wall. For large values of the Rayleigh number a stratification of the temperature near the same wall can be seen (Figs. 4 and 5).

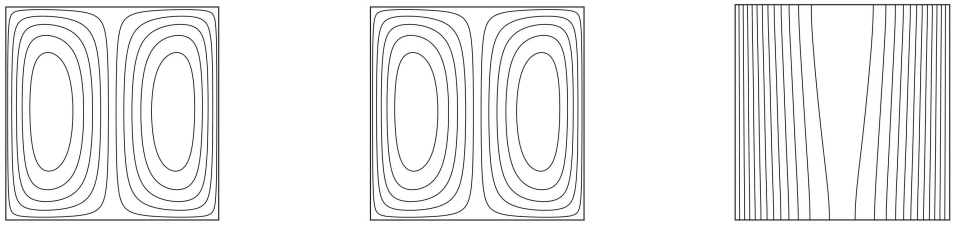

(a) $\max|\psi_f| = 0.6698$ (b) $\max|\psi_p| = 0.0788$ (c) $\max|\Theta| = 0.1304$

Figure 2: Streamlines for (a) macrophase, (b) microphase and (c) isotherms for $Ra = 10^2$, $Kr = 0.1$, $\sigma_f = 0.1$

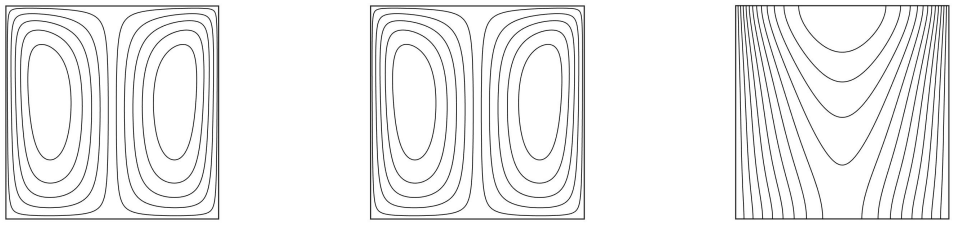

(a) $\max|\psi_f| = 4.9773$ (b) $\max|\psi_p| = 0.5855$ (c) $\max|\Theta| = 0.1262$

Figure 3: Streamlines for (a) macrophase, (b) microphase and (c) isotherms for $Ra = 10^3$, $Kr = 0.1$, $\sigma_f = 0.1$

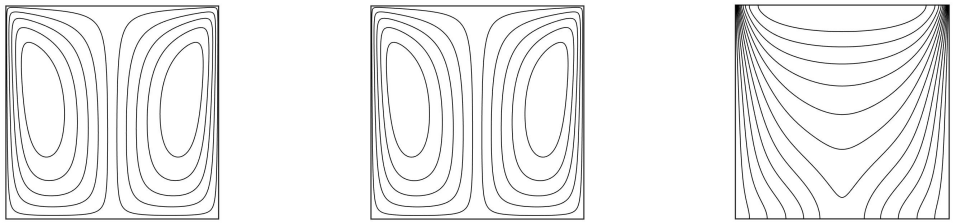

(a) $\max|\psi_f| = 13.9690$ (b) $\max|\psi_p| = 3.4922$ (c) $\max|\Theta| = 0.0778$

Figure 4: Streamlines for (a) macrophase, (b) microphase and (c) isotherms for $Ra = 10^4$, $Kr = 0.1$, $\sigma_f = 0.1$

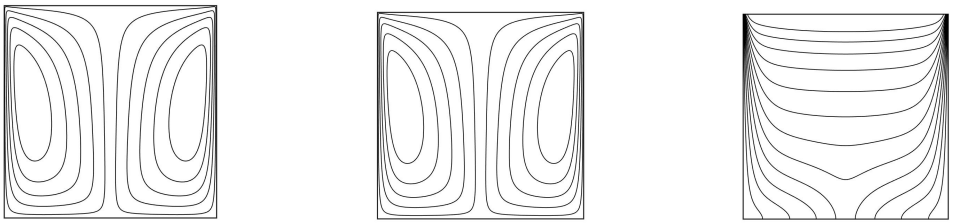

(a) $\max|\psi_f| = 39.9481$ (b) $\max|\psi_p| = 9.9870$ (c) $\max|\Theta| = 0.0368$

Figure 5: Streamlines for (a) macrophase, (b) microphase and (c) isotherms for $Ra = 10^5$, $Kr = 0.1$, $\sigma_f = 0.1$

**Acknowledgements.** This study was supported from the grant PN-III-P4-PCE-2021-0993 (contract PCE 69/2022), UEFSCDI, Romania

## References

[1] D. Bufnea, V. Niculescu, Gh. Silaghi, A. Sterca, *Babeş-Bolyai University's high performance computing center*, Studia Univ. Babeş-Bolyai Inform., 61 (2016), 54—69.

[2] M. Haajizadeh, A.F. Ozguc, C.L. Tien, *Natural convection in a vertical porous enclosure with internal heat generation*, Int. J. Heat Mass Transfer 2 (1984), 1893–1902.

[3] G. Imani, K. Hooman, *Lattice Boltzmann pore scale simulation of natural convection in a differentially heated enclosure filled with a detached or attached bidisperse porous medium*, Transp. Porous Med 116 (2017), 91–113.

[4] M. Gentile, B. Straughan, *Bidispersive thermal convection*, Int. J. Heat Mass Transfer, 114 (2020), pp. 837—840.

[5] T. Groşan, C. Revnic, I.Pop, D.B. Ingham, *Magnetic field and internal heat generation effects on the free convection in a rectangular cavity filled with a porous medium*, Int. J. Heat Mass Transfer, 52 (2009), 1525–1533.

[6] D.A. Nield, A. Bejan, *Convection in Porous Media*, 5th ed., Springer, New York, 2017.

[7] D.A. Nield, A.V. Kuznetsov, *Heat transfer in bidisperse porous media*, in Ingham, D.B. and Pop, I. (Ed.s), Transport in Porous Media, Vol. III, Elsevier, Oxford (2005), 34—59.

[8] B. Straughan, *Convection with Local Thermal Non-Equilibrium and Microfluidic Effects*, Springer, Heidelberg, 2015.

[9] D.A.S Rees, D.A. Nield, A.V. Kuznetsov, *Vertical free convective boundary-layer flow in a bidisperse porous medium*, ASME J. Heat Transfer 130 (2008), 092601.

[10] C. Revnic, T. Groşan, I. Pop, D.B. Ingham, *Free convection in a square cavity filled with a bidisperse porous medium*, Int. J. Thermal Sci. 48 (2009), 1876–1883.

[11] F.O. Pătrulescu, T. Groşan, I. Pop, *Natural Convection from a vertical plate embedded in a non-Darcy bidisperse porous medium*, J. Heat Transfer 142, 1 (2020), 012504.

[12] Ke. Wang, Q. Wang, P. Li, *Forced convection in a fully-filled bidisperse porous annular duct subject to asymmetric heat fluxes*,Therm. Sci. Eng. Progress 32, 1 (2022), 101328.

Daniel Breaz
Facultatea de Stiinte Exacte si Ingineresti,
Universitatea *1 Decembrie 1918* din Alba Iulia,
Alba Iulia, Romania
email: *dbreaz@uab.ro*

Teodor Groşan
Department of Mathematics, Faculty of Mathematics and Computer Science,
Babes-Bolyai University,
Cluj-Napoca, Romania
email: *teodor.grosan@ubbcluj.ro*

Flavius Pătrulescu
Department of Mathematics
Technical University of Cluj-Napoca
Cluj-Napoca, Romania
email: *Flavius.Patrulescu@math.utcluj.ro*

Cornelia Revnic
Faculty of Pharmacy
University of Medicine and Pharmacy
Cluj-Napoca, Romania
email: *cornelia.revnic@umfcluj.ro*